Chaos, Solitons and Fractals 134 (2020) 109677

Contents lists available at ScienceDirect

Chaos, Solitons and Fractals

Nonlinear Science, and Nonequilibrium and Complex Phenomena

journal homepage: www.elsevier.com/locate/chaos

Noise-induced kink propagation in shallow granular layers

Gladys Jara-Schulz*, Michel A. Ferré, Claudio Falcón, Marcel G. Clerc

Departamento de Física, Facultad de Ciencias Físicas y Matemáticas, Universidad de Chile, Casilla 487-3, Santiago, Chile

ARTICLE INFO

Article history:
Received 25 October 2019
Revised 23 January 2020
Accepted 31 January 2020
Available online 3 March 2020

ABSTRACT

Out of equilibrium systems are characterized by exhibiting the coexistence of domains with complex spatiotemporal dynamics. Here, we investigate experimentally the noise-induced domain wall propagation on a one-dimensional shallow granular layer subjected to an air flow oscillating in time. We present results of the appearance of an effective drift as a function of the inclination of the experimental cell, which can be understood using a simple Langevin model to describe the dynamical evolution of these solutions via its pinning-depinning transition. The statistical characterization of displacements of the granular kink position is performed. The dynamics of the stochastic model shows a fairly good agreement with the experimental observations.

1. Introduction

A characteristic of out of equilibrium nonlinear systems is the coexistence of different equilibria, i.e. *multistability*. Namely, depending on initial conditions, different equilibria can be observed [1–4]. One of the simplest systems that shows coexistence of stable states is the bistable model [1–4]. To describe the spatial variations of physical systems one can couple single units of the above model elastically with their nearest neighbors and recover the dissipative ϕ^4-model field equation [5]. The dissipative ϕ^4-model has been succesfully used to study magnetic textures, high energy and particle physics, and optical systems to mention a few [5–7]. Considering different inhomogeneous initial conditions, the model above exhibits the emergence of different domains separated by walls or defects [6,7]. Each domain accounts for one of the original (homogeneous) equilibria that spans a portion of the extended system. That is, wall account for the spacial region that connects the differents equilibria, *interface*. The wall dynamics depicts the most favorable state invading the least favorable one [8]. Generally, when one changes a control parameter, the relative stability of the equilibria can also change. In this context, there is a unique value of the control parameters for which a flat wall remains motionless, called the Maxwell point [9]. In two spatial dimensions, the wall or interface connecting two symmetrical states will also move as it tries to decrease its local curvature [10]. This phenomenon is well-known in the literature as Gibbs-Thomson effect [10]. This scenario of wall dynamics changes drastically in one spatial dimension, where the interaction between walls drives the domain dynamics [11]. Domain walls that connect symmetric states in one spatial dimension are usually referred to as kinks. Their interaction decaying exponentially depends on the distance between domains. Due to the attractive interaction of nearby kinks, the dynamics of a kink gas tends to homogenize the system. Displaying as its ultimate equilibrium a homogeneous state [11]. However, the previous evolution is difficult to observe experimentally and numerically since the walls remain motionless as a result of experimental imperfections or inherent dicretization of numerical simulations.

Another crucial ingredient in the dynamics of the domain walls—due to the macroscopiv nature of experiments—are the inherent fluctuations of the physical systems under study, i.e. noise. Theoretically, the effects of noise are included by considering stochastic terms in partial differential equations [12]. In the case of a wall that connects two symmetric states in one-dimension, it is expected that as a result of the inherent fluctuations that the position of the wall or defect will perform a random one-dimensional motion [13].

In the case that the walls separate a homogeneous domain with a spatial one (pattern), the interface dynamics changes radically as the pattern breaks the spatial translation symmetry. As a consequence of this change, the wall propagation exhibits spatially periodic leaps [8]. The wall or defect remains motionless in a range of parameters close to the Maxwell point, *pinning range*, as a result of the translation breaking symmetry. That is, although one state is less stable than the other, the system remains motionless and no propagation of the most stable state over the other one is observed. The origin of this phenomenology is because the pattern induces a nucleation barrier over the dynamic of domain walls [14,15]. Experimentally this scenario has been verified in a liquid crystal light valve with optical spatial modulation feedback [16]. The inclusion of inherent fluctuations causes the domain wall on

* Corresponding author.
E-mail address: gjara.schulz@gmail.com (G. Jara-Schulz).

https://doi.org/10.1016/j.chaos.2020.109677
0960-0779/

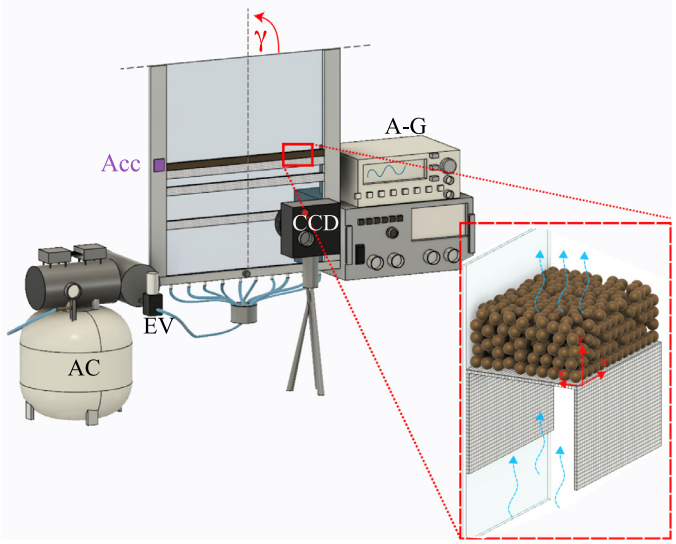

Fig. 1. (Color online) Schematic diagram of the experimental setup. AC accounts for the air compressor, EV is the electromechanical valve, A-G stand for the amplifier and function generator, γ is the inclination angle of the Hele-Shaw cell (HS) measured with MEMS accelerometer (Acc). Inset: Granular layer arrangement on top of the metallic mesh which serves a porous floor. Arrows depict flow direction.

average to advance towards a flank, so that the most stable state is propagated onto the least stable. This phenomenon is known as noise induces front propagation [14,15]. Namely, noise is the driving of domain wall propagation. This phenomenon can be understood as a Brownian motor [17], that is, considering a particle in an unbounded asymmetric potential with periodic equilibria under random fluctuations [14,15]. However, noise induces front propagation has only been studied theoretically. A good candidate to observe such a phenomenon is a one-dimensional experimental setup that exhibits parametric instability that give rise to domain walls between standing waves with relevant inherent fluctuations is a one-dimensional shallow granular layer subjected to an airflow oscillating in time [19,20].

The present work aims to investigate how noise induces front propagation experimentally. Based on a fluidized quasi-one-dimensional shallow granular bed, the dynamics of walls or defects, called granular kinks, is characterized. The fluidization process is driven by a time-periodic airflow, which corresponds to a tapping-type forcing on the granular layer subjected to gravity. These granular kinks connect two symmetrical states [19,20], which display an underlying pattern depending on the experimental parameters of the system. By slightly tilting the cell, the relative stability between the granular domains can be controlled. As a result of granular fluctuations and cell inclination, the granular kink moves and its propagation speed exhibits different dynamical behaviors. Two regimes are identified, one associated with pinning and another with drifting. In the former, granular kinks exhibit long-waited fluctuations and propagate slowly through spatially periodic leaps. In the latter, granular kinks propagate quickly with small fluctuations and a large drift. The statistical characterization of the displacement of the granular kink position is also performed. Theoretically, an over-damped particle in a washboard potential with additive noise [18] models the position of the granular kink. The dynamics of this Langevin equation shows a fairly good agreement with the experimental observations.

2. Experimental setup and measurement techniques

The experimental setup is depicted in Fig. 1. An aluminium frame encases two large glass walls 250 mm wide, 320 mm tall and 35 mm in depth (Hele-Shaw cell), with an horizontally placed porous steel mesh that serves as a porous floor where approximately 27,000 monodisperse bronze spheres (diameter $d = 350\,\mu$m) are deposited, forming a shallow granular layer. The layer is thus is approximately $400d$ long, $10d$ deep, and $5d$ tall. The granular layer is subjected to a time-periodic driving (similar to the ones described in [19–23]), via an modulated air flow which is generated by an air compressor and regulated by an electromechanical proportional valve. The valve opens and closes following a variable voltage signal sent by a function generator through a power amplifier. A symmetrical sinusoidal signal with frequency f_o and a non-zero offset is used to generate the air flow. As in previous studies [19–23], a linear dependence is found between the peak voltage delivered by the function generator and the peak pressure fluctuations P_o oscillating at f_o. This experimental cell can be inclined horizontally with an angle γ, measured by a MEMS (microelectromechanical systems) accelerometer glued to the cell. Off-plane inclinations are forbidden as the cell is mounted on an in-house aluminium bearing, ensuring only in-plane rotations of the whole cell. Hence, in our experiments, the control parameters are f_o, P_o, and γ.

Images of the granular layer's spatial dynamics are acquired using a CCD camera placed 10 cm away from the cell about 600 s time window in a 780×200 pixel interrogation window with a 78 pixel/cm sensitivity and later stored on a PC, to be digitally analyzed using Matlab. The acquisition frequency was set at $f_o/2$. The layer is illuminated from the back with white light through a diffusing screen in order to enhance the contrast between the motion of the grains and their background. The surface fluctuations of the granular layer are computed for every point x in space at each time step t using a front-tracking algorithm similar to the one used in [22]. A typical snapshot of the tracking scheme's output is shown in Fig. 1(a).

3. Granular kinks dynamics

Before initiating dynamical measurements, the acquired value of γ is corroborated with a series of images of the experimental cell acquired with a CCD camera without any driving. Then, for a given f_o, we increase P_o generating spontaneously small fluctuations of the granular layer's interface (of the order of d). This motion increases with P_o up to the point where the entire layer is lifted by the drag force generated by the air flow which can overcome the layer's weight. This motion is periodic and its period is $1/f_o$. The dynamics of the homogeneous layer changes qualitatively at a critical value $P_o = P_o^c$ where the flat oscillating layer becomes unstable through an effective supercritical parametric instability, displaying subharmonic oscillations at $f_o/2$ [19,20] and, thus, the possibility of the spatial connection between two spatially homogeneous equilibria (one oscillating in-phase with the driving and one oscillating out-of-phase with the driving) which is called kink. The granular kink, as a function of frequency f_o and pressure P_o, exhibits a parametric instability as the pressure increases or the frequency decreases [19]. Hence, inhomogeneities due to noisy initial conditions give rise to domain walls. Granular kinks are robust to changes in f_o (which sets its oscillating frequency) and $\Delta P_o = P_o^c - P_o$ (which sets its amplitude). To characterize the dynamics of kink as a particle-type state, one can identify a peculiar position. We introduce the kink position $x_o(t)$ as the intermediate point that separates the two domains, which corresponds to the position with the most significant spatial variation of the kink profile. Fig. 2 depicts the granular kink position in a given time and the typical spatiotemporal evolution of the kink (see the video on Supplementary Material [24]). Due to the discrete and finite nature of the constituents of the granular medium, the profile of granular kink exhibits significant fluctuations. Likewise, one can identify

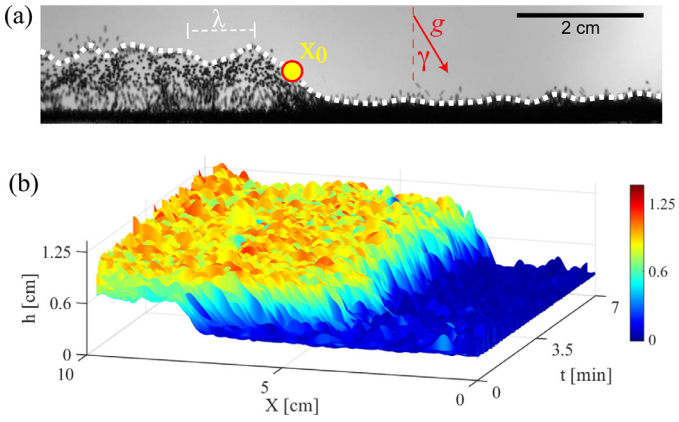

Fig. 2. (Color online) Granular kink. (a) Snapshot of a kink profile for $P_o = 7$ kPa, $f_o = 14$ Hz, and $\gamma = 0.4°$. The granular kink position x_o is depicted by a circle (○) and λ accounts for the characteristic wavelength of the oscillatory domains. g stands for the gravity. White dashed line shows the kink profile. (b) Spatiotemporal diagram of the propagating kink for the same parameters as in (a).

that domains are characterized by exhibiting a well-defined wavelength λ (cf. Fig. 2). For each period, we compute λ by taking the instantaneous fast Fourier transform of the dilated domain of the granular layer's profile and averaging it over 6000 iterations. Thus, λ corresponds to the inverse of the wave number at which this average attains its maximum. This wavelength is responsible for the nucleation barrier for main wall dynamics [14,15].

In the case of a horizontal cell $\gamma = 0$, $x_o(t)$ has been shown to follow a hopping-type of motion, where the characteristic hopping length is determined by lambda [19,20], much similar to the dynamics of a Brownian particle in a periodic potential [17,25]. In the center left panel of Fig. 3 a spatiotemporal diagram of the kink evolutions is depicted showing a Brownian-type dynamics. The intrinsic fluctuations of the granular layer, averaged over the typical size of the kink, give rise to an effective noise term that drives the Brownian-type evolution of $x_o(t)$, allowing the kink to move back and forth randomly around its initial position. When $\gamma \neq 0$, the dynamics of the granular kink position $x_o(t)$ depicted above changes qualitatively and quantitatively as the granular layer becomes inhomogeneous due to gravity (see Fig. 2a). In what follows, we focus on the dependence of the cell inclination γ on the kink dynamics by studying the temporal evolution of the granular kink position $x_o(t)$.

Varying the cell inclination γ between $[-1, 1]°$, with an angle step $\Delta\gamma = 0.2°$ as we fix the forcing frequency $f_o = 14$ Hz and pressure $\Delta P_o = 100$ Pa with $P_o = 70$ kPa. As the cell is not horizontal $|\gamma| > 0$, the granular kink position $x_o(t)$ displays also a fluctuating dynamics, but with a well defined mean propagation velocity $\langle v \rangle = \langle \dot{x}_o(t) \rangle \neq 0$ and thus the granular kink moves towards the left ($\gamma > 0$) or the right ($\gamma < 0$) *deterministically*. Random fluctuations are also present as they arise from intrinsic granular fluctuations. This means that the typical trajectory of $x_o(t)$ is highly fluctuating with a non-zero mean drift, depending solely on γ. This is shown in Fig. 3(Left), where typical spatiotemporal diagrams of the kink dynamics are depicted for negative, zero, and positive values of γ. $\langle v \rangle$ is experimentally found by averaging over several trajectories for fixed f and ΔP_o at a given γ. A non-zero $\langle v \rangle$ is found for all $\gamma \neq 0$, where error bars stand for standard deviations. The central panel in Fig. 3 summarizes the average speed of granular kink as a function of the cell inclination. From this chart we infer that $\langle v \rangle$ exhibits different dynamical behaviors. Two regime are identified, one characterized by granular kinks displaying large spatial fluctuations propagating slowly (region valid for small angles, $|\gamma| < 0.25°$). In the other regime, the granular kinks propagate quickly with small fluctuations. In this last regime, the speed increases linearly with the cell inclination. Then, we have term this behavior as drifting.

4. Theoretical model for the granular kink position

Despite having a detailed description of the granular microscopic dynamics, to date, there is no established hydrodynamic-type macroscopic model to account for the driven granular phenomena [26–28]. That is, we do not have a continuous model from which we can infer the existence of a parametric instability that generates domain walls between standing waves. Based on the Goldstone mode theory and solubility conditions [10], one expects that from a continuous model an equation for the granular kink position can be derived [14,15,29]. Because the domain wall connects steady wave patterns, one expects that the kink position satisfies an equation of an overdamped particle in a washboard potential with additive noise.

For simplicity, let us consider the following Langevin equation for granular kink position

$$\dot{x}_o = \Gamma + A\cos\left(\frac{\pi}{2\lambda}x_o\right) + \sqrt{\eta}\zeta(t), \tag{1}$$

where Γ accounts for cell inclination, A stands for the threshold induced by the periodic potential, η is the intensity level of noise, and $\zeta(t)$ is a Gaussian $\delta-$correlated white noise with zero mean value. The dynamics of the front between homogeneous and periodic solutions in the context of pattern formation the Lagevin Eq. (1) has been rigorously derived [14,15]. In the context of liquid crystals lifht valve with modulated optical feedback, Eq. (1) was derived without noise to describe the front dynamics [16]. In addition, similar model was also derived in wall domains between standing waves [29] and front between uniform and pattern state under deterministic fluctuations [32]. The model Eq. (1) has been fundamental to understand the pinning-deppining transition [33].

Analytical solutions of Eq. (1) when $A \neq 0$ are unknown. Thus, we have considered numerical simulations as a strategy of study this stochastic model. Fig. 3 summarizes the results found for the average speed $\langle \dot{x}_o \rangle = \langle v \rangle$, which shows a good agreement with the experimental observations. To understand this behavior, one can first track the dynamics of the deterministic system, i.e. for $\eta = 0$. For $|\Gamma/A| \leq 1$, the model Eq. (1) exhibits periodic equilibria of the form $x_o^* = \arccos(\Gamma/A)$. Hence, in this range of parameters of the cell inclination the granular kink without fluctuations is motionless. Thus, the granular kink is in the pinning range. In the central panel of Fig. 3, the horizontal solid segment accounts for the pinning region. For $|\Gamma/A| > 1$, the system does not have equilibria and then the position of the granular kink propagates with a well defined mean speed, oscillating in time. Analytically, one can determine the expression for the average speed, which reads [31]

$$\langle \dot{x}_o \rangle = \begin{cases} \sqrt{\Gamma^2 - A^2}, & |\Gamma/A| > 1 \\ 0 \quad , & |\Gamma/A| < 1 \end{cases} \tag{2}$$

Then, close to and far from the end of the pinning region, the average speed grows with the square root of Γ/A and linearly with Γ/A, respectively, due to the saddle-node bifurcation. The solid curve of Fig. 3 depicts the expression (2). The inclusion of noise causes the deformation of this curve as now there is only one point where the average speed is zero, the Maxwell point [9]. Fig. 1 shows the average speed obtained from Eq. (1) by adjusting the intensity of noise level and Γ parameter and compares it to the experimentally found curve. Note that we find that $\Gamma = \gamma - \gamma_o$ (where $\gamma_o = 0.2$); therefore, the Maxwell point does not correspond to the horizontal cell inclination. This is due to the fact that experimental setup has a small angular ofset stemming from the slight inclination of the steel mesh used to support the

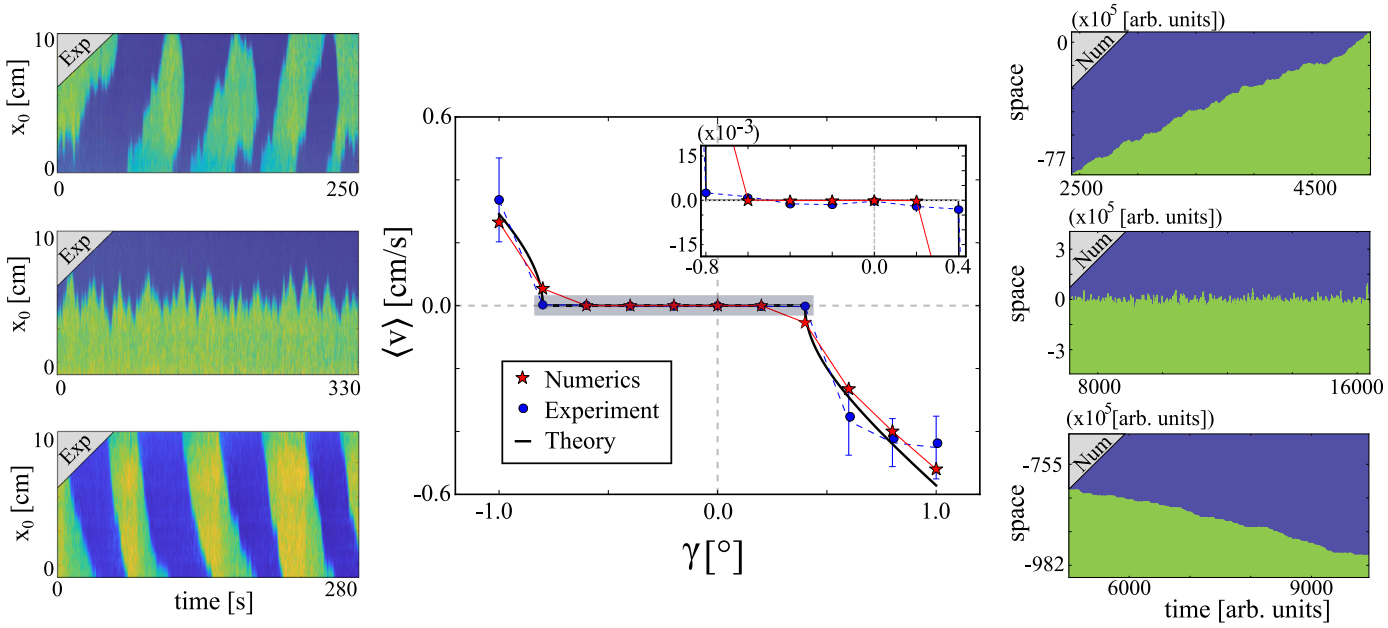

Fig. 3. (Color online) Noise-induced kink propagation in shallow granular layers. *Left:* Experimental spatiotemporal diagram of the propagating kink for $P_o = 7$ kPa, $f_o = 14$ Hz and $\gamma = -1.0^\circ$ (top), 0.2° (center), and 1.0° (bottom). *Center:* Average kink speed $\langle v \rangle$ vs the cell inclination γ. Experimental ($\circ$) data is compared with numerics ($\star$) from Eq. (1). The continuous line is the average speed obtaining from the deterministic model Eq. (3) by $\Gamma = \gamma - \gamma_0$, $\gamma_o = 0.2$, $\lambda = 0.24$, $A = 0.7$, and $\eta = 10$. Error bars stand for the standard deviation of the granular kink speed. Inset accounts for a magnification of the pinning region. *Right:* Numerical spatiotemporal diagram of the propagating kink for Eq. (1) and $\gamma = -1.0$ (top), $\gamma = 0.0$ (center) and $\gamma = 1.0$ (bottom).

granular layer with respect to the aluminium frame. Likewise, we note that the speed of granular kink is not symmetric with respect to the inclination of the cell. Note that the noise level is large.

From the above plot, we conclude that for small cell inclinations ($\gamma \leq 1^\circ$) the granular kink propagates due to the fluctuations in a noisy pinning region. That is, the granular kink presents large fluctuations and propagate slowly. For greater cell inclination, the mechanism of propagation of the granular kink is due to the drift generated by gravity, i.e. the drifting regime, where the granular kink propagates quickly with small fluctuations. In addition, the average speed of granular kink grows roughly linearly with the inclination of the cell.

5. Statistical characterization of granular kink dynamics

In Ref. [30], a detailed analytical study of the conditional and stationary probability is presented for the Brownian motion in a washboard potential of Eq. (1) assuming a constant flow of probability. However, under the conditions of our experiment, the mathematical assumptions are not fulfilled and then this type of analysis does not suit our experimental configuration.

The statistical characterization of the displacement of the granular kink position $\Delta x(t) = x_o(t + \Delta t) - x_o(t)$ is performed. Here Δt is the temporal interval between measurements ($\Delta t = 0.1$ in numerics and $\Delta t = 2/f_o$ in experiments). Unlike the position of the granular kink (which does not have a stationary distribution) the displacement of granular kink does have a stationary distribution [30]. Fig. 4(a) show the numerically (left) and experimentally (right) computed temporal evolution of granular kink displacement at given cell inclination $\gamma = -1.0^\circ$. As a result of the inclination, the kink displays more displacements towards the right flank than towards the left one. The panels in Fig. 4(b) show the respective probability distributions functions (PDFs) of the granular kink displacements. For small cell inclination, we observe a stationary distribution which is well described by a Gaussian. As the cell inclination increases, the probability distribution is deformed asymmetrically, so that the maximum moves in opposition to the direction of the inclination. Fig. 4(d) summarize the evolution of a probability density distribution as a function of the cell inclination. Note that the probability of displacement distribution in the pinning region is a slightly deformed Gaussian with a small width, but in the drifting region, the probability density distribution width is much larger. This is a consequence of the fact that in the drifting region the granular kink performs large displacements.

To figure out the complexity of the dynamics exhibited by the temporal evolution of granular kink displacement we have calculated the power spectral density (PSD) of $\Delta x(t)$. Panels of Fig. 4(c) illustrate the respective power spectrum density. These spectra are characterized by being approximatively flat in a wide frequency range, which manifests the random dynamics of the displacements. Numerically, the spectra show a peak for low frequencies related to the typical drifting frequency $\langle v \rangle / \lambda$ when the kink is in the drifting regime. For larger frequencies the spectra are flat. Experimentally, a similar trend is observed. The only differences are that the width of the peak is much larger than in the case of the numerical simulations and that the flat frequency level of the PSD depends on the inclination, which shows a certain anisotropy of the local fluctuations of the granular layer.

6. Conclusions and remarks

Brownian motors are relevant machines at nanometric scales, where the conversion of random movement into mechanical work on living systems. Here we have reported that a quasi-one-dimensional domain wall out of equilibrium can propagate in a given direction as a result of the inherent fluctuations. Indeed, a prerequisite for observing this type of phenomenon is that: i) one of the domains displays a characteristic length scale and ii) the domains are not symmetrical. Based on a one-dimensional shallow granular layer subjected to an temporally oscillating airflow, granular kinks are observed as a result of parametric instability. Granular walls separate two symmetric standing waves subjected to sharp fluctuations. The dynamics of the domain wall is characterized by exhibiting a random hopping walk. By tilting the exper-

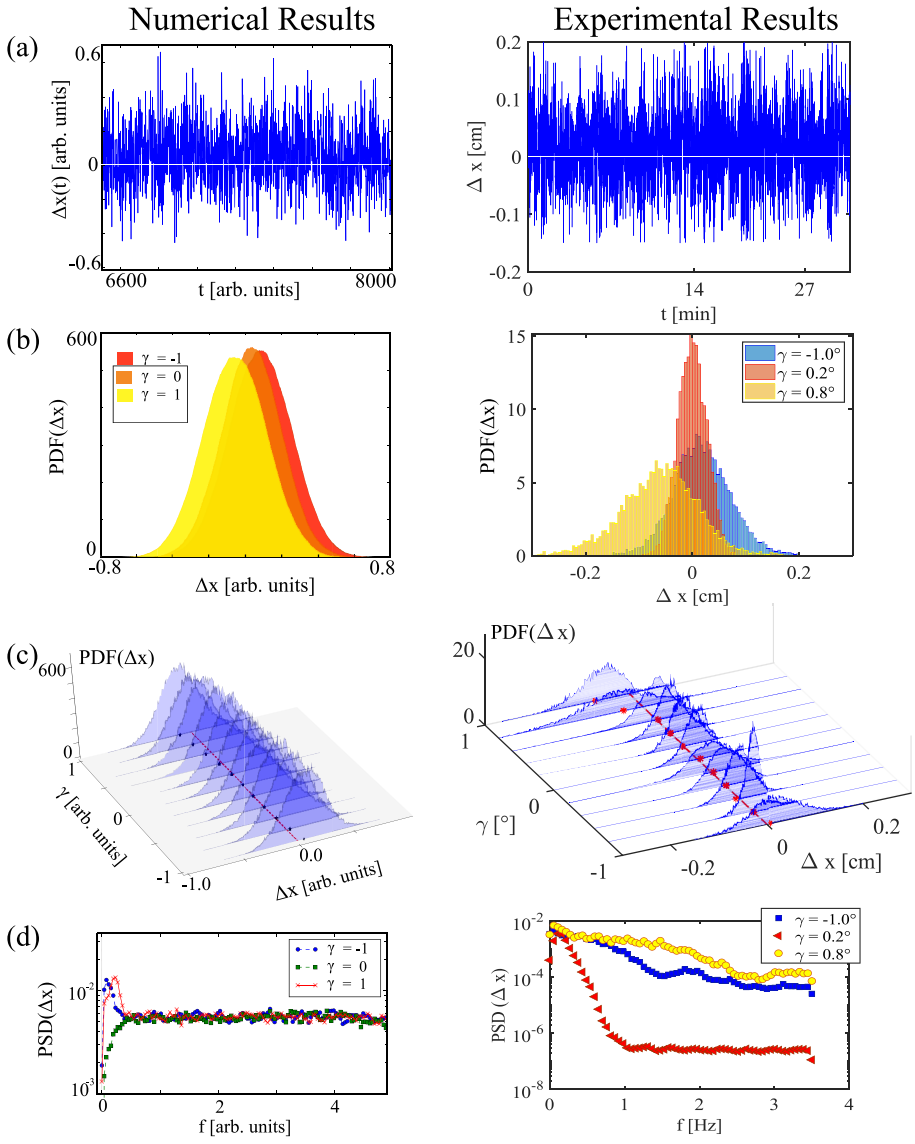

Fig. 4. (Color online) Statistical characterization of granular kink dynamics. Left column for numerical simulations and right column for experimental data. (a) Displacement for propagating kink for $P_o = 7$ kPa, $f_o = 14$ Hz and $\gamma = -1.0^\circ$. (b) Displacement histograms for different angles. (c) Displacement PDF for all angles from -1.0° until 1.0° with an angle step $\Delta\gamma = 0.2^\circ$. The red asterisk points out the maximum value for the each PDF. (d) Displacement PSD for the same angles in (b).

imental setup, the symmetry of the domains can be broken, which induces a ratchet potential for the domain wall. Indeed, one domain is energetically more favorable than the other. Therefore for small angles of cell inclination, noise induces the propagation of the granular kink. When the angle of the cell inclination is large enough, the domain walls drift in the direction that minimizes energy. Fluctuations can induce a new wall domain, which again propagates (cf. left bottom panel of Fig. 3). The possibility of manipulating the cell inclination allows us to control the propagation of kink (both direction and magnitude). The effect of the larger non-linearities on kink propagation as the amplitude of the granular pattern increases is still not well understood, and further work in that direction is needed.

Declaration of Competing Interest

The authors declare that they have no known competing financial interests or personal relationships that could have appeared to influence the work reported in this paper.

CRediT authorship contribution statement

Gladys Jara-Schulz: Investigation, Data curation, Visualization, Software, Writing - review & editing. **Michel A. Ferré:** Software, Formal analysis, Writing - review & editing, Visualization. **Claudio Falcón:** Validation, Methodology, Writing - review & editing, Resources. **Marcel G. Clerc:** Conceptualization, Supervision, Project administration, Methodology, Validation, Writing - review & editing, Formal analysis.

Acknowledgments

This work was supported by CONICYT-USA PII20150011. G.J.S., M.G.C., and M.A.F. also thank the Millennium Institute for Research in Optics (MIRO) and Fondecyt 1180903 for financial support.

Supplementary material

Supplementary material associated with this article can be found, in the online version, at 10.1016/j.chaos.2020.109677

References

[1] Nicolis G. Introduction to nonlinear science. Cambridge: Cambridge University Press; 1995.
[2] Jackson EAE. Perspectives of nonlinear dynamics, vol. 1 and 2. Cambridge: Cambridge University Press; 1989.
[3] Strogatz SH. Nonlinear dynamics and chaos: with applications to physics, biology, chemistry, and engineering. CRC Press; 2018.
[4] Guckenheimer J, Holmes P. Local bifurcations. In nonlinear oscillations, dynamical systems, and bifurcations of vector fields. New York: Springer; 1983.
[5] Kleinert H, Schulte-Frohlinde V. Critical properties of ϕ 4-theories. Singapore: World Scientific; 2001.
[6] Manton N, Sutcliffe P. Topological solitons. Cambridge: Cambridge University Press; 2004.
[7] Vachaspati T. Kinks and domain walls: an introduction to classical and quantum solitons. Cambridge: Cambridge University Press; 2006.
[8] Pomeau Y. Front motion, metastability and subcritical bifurcations in hydrodynamics. Phys D 1986;23:3–11.
[9] Goldstein RE, Gunaratne GH, Gil L, Coullet P. Hydrodynamic and interfacial patterns with broken space-time symmetry. Phys Rev A 1991;43:6700.
[10] Pismen LM. Patterns and interfaces in dissipative dynamics. Berlin Heidelberg: Springer Series in Synergetics; 2006.
[11] Kawasaki K, Ohta T. Kink dynamics in one-dimensional nonlinear systems. Phys A 1982;116:573–93.
[12] García-Ojalvo J, Sancho J. Noise in spatially extended systems. Springer Science & Business Media; 2012.
[13] Funaki T. The scaling limit for a stochastic PDE and the separation of phases. Probab Theory Relat Fields 1995;102:221288.
[14] Clerc MG, Falcon C, Tirapegui E. Additive noise induces front propagation. Phys Rev Lett 2005;94:148302.
[15] Clerc MG, Falcon C, Tirapegui E. Front propagation sustained by additive noise. Phys Rev E 2006;74:011303.
[16] Haudin F, Elias E, Rojas RG, Bortolozzo U, Clerc MG, Residori S. Driven front propagation in 1d spatially periodic media. Phys Rev Lett 2009;103:128003.
[17] Astumian RD, Hänggi P. Brownian motors. Phys Today 2002;55(11):33–9.
[18] Costantini G, Marchesoni F. Threshold diffusion in a tilted washboard potential. EPL 1999;48:491.
[19] Macías JE, Clerc MG, Falcón C, García-Ñustes MA. Spatially modulated kinks in shallow granular layers. Phys Rev E 2013;88:020201(R).
[20] Macías JE, Falcón C. Dynamics of spatially modulated kinks in shallow granular layers. New J Phys 2014;16:043032.
[21] Macías JE, Clerc MG, Falcón C. Dynamics of a one-dimensional kink in an air-fluidized shallow granular layer in nonlinear dynamics: materials, theory and experiments. In: Tlidi M, Clerc M, editors. Springer proceedings in physics, 173. Cham: Springer; 2016.
[22] Ortega I, Clerc MG, Falcon C, Mujica N. Subharmonic wave transition in a quasi-one-dimensional noisy fluidized shallow granular bed. Phys Rev E 2010;81:046208.
[23] Garay J, Ortega I, Clerc MG, Falcón C. Symmetry-induced pinning-depinning transition of a subharmonic wave pattern. Phys Rev E 2012;85:035201(R).
[24] See Supplementary Material for a movie that shows the granular kink propagation.
[25] Reiman P, Hanggi P. Introduction to the physics of Brownian motors. Appl Phys A 2002;75:169.
[26] Aronson I, Tsimring L. Granular patterns. New York: Oxford University Press; 2009.
[27] Andreotti B, Forterre Y, Pouliquen O. Granular media: between fluid and solid. New York: Cambridge University Press; 2013.
[28] Goddard JD. Mathematical models of granular matter. Berlin Heidelberg: Springer; 2008.
[29] Clerc MG, Fernández-Oto C, Coulibaly S. Pinning-depinning transition of fronts between standing waves. Phys Rev E 2013;87:012901.
[30] Risken H. Fokker-planck equation. Berlin, Heidelberg: Springer; 1996.
[31] Rojas R.. Sur de gouttes, cristaux liquides et fronts [dissertation] University of Nice Sophia Antipolis. France. See http://tel.archives-ouvertes.fr.
[32] Alvarez-Socorro AJ, Clerc MG, Ferré MA, Knobloch E. Front depinning by deterministic and stochastic fluctuations: a comparison. Phys Rev E 2019;99:062226.
[33] Bensimon D, Shraiman BI, Croquette V. Nonadiabatic effects in convection. Phys Rev A 1988;38(10):5461.